

Transition from Spirals to Defect-Mediated Turbulence Driven by a Doppler Instability

Qi Ouyang,^{1,*} Harry L. Swinney,^{2,†} and Ge Li²

¹*Department of Physics, Mesoscopic Physics Laboratory, Peking University, Beijing 100871, China*

²*Center for Nonlinear Dynamics and Department of Physics, The University of Texas at Austin, Austin, Texas 78712*

(Received 9 August 1999)

A transition from rotating chemical spirals to turbulence is observed in experiments on the Belousov-Zhabotinsky reaction. The transition occurs when the waves near the spiral tip spontaneously break, generating defects. Measurements reveal that this defect-mediated turbulence is caused by the Doppler effect on the traveling waves. The observations are in good accord with numerical simulations and theory.

PACS numbers: 82.40.Ck, 47.54.+r, 82.20.Mj, 87.19.Hh

Rotating spiral waves generated by self-organized rotors in spatially extended systems occur in various excitable media including bacterial colonies [1], cardiac muscle [2], and reaction-diffusion media [3]. Studies on animal hearts show that the birth, death, and motion of spiral waves are closely related to reentrant excitation, which causes life-threatening situations such as tachycardia and fibrillation [2,4–9]. One proposed mechanism for the onset of cardiac fibrillation is that it arises from defect-mediated turbulence which occurs when spiral rotors (defects) are spontaneously generated [4–6]. Here we present an experimental observation of such a defect-generating process in a reaction-diffusion system with Belousov-Zhabotinsky (BZ) kinetics. The observed spiral instability occurs when the spiral tip meanders and the Doppler effect becomes so large that adjacent waves interact and break, forming defects. Our observations are in accord with a mechanism of defect-mediated turbulence which was proposed by Bär *et al.* [10].

The Doppler mechanism described here differs from two other mechanisms that have been found to generate defect-mediated turbulence: the Eckhaus instability [11], which occurs in a nonexcitable medium where spiral waves are phase waves, and the line instability [12], which requires an external periodic perturbation. The latter mechanisms do not account for cardiac fibrillation [13], while the Doppler effect we have observed provides a plausible mechanism for fibrillation.

Our study of the asymptotic behavior of spiral waves and their stability is conducted in a quasi-two-dimensional open reactor [14] with a ferroin-catalyzed BZ reaction. The reaction medium is a thin porous glass disk, 0.4 mm thick and 19.6 mm in diameter (Vycor glass, Corning). The porous glass, which has about 25% void space and 100 Å average pore size, prevents convective motion in the disk, allowing only reaction and diffusion processes to occur. The opposite faces of the porous glass disk are, respectively, in contact with two reactant reservoirs A and B (each 6.6 ml in volume), where the reactant concentrations are kept constant and uniform by appropriate mixing and continuous pumping of fresh reactants. The components of the BZ reaction are asymmetrically distributed in

the two reservoirs: malonic acid ($[\text{CH}_2(\text{COOH})_2]_0$) and potassium bromide are fed only in reservoir A; ferroin and sulfuric acid are fed only in reservoir B. Sodium bromate is contained in equal amounts in each reservoir. The reactants diffuse from both sides into the porous glass where the pattern-forming reaction occurs, and opposing chemical concentration gradients form in the direction normal to the plane of reaction medium. The surface in contact with chemicals in reservoir A is made slightly larger than that in contact with reservoir B; this prevents the spontaneous generation of chemical waves from the boundary. The control parameter in our experiments is the concentration of malonic acid.

The initial condition is chosen so that only one spiral rotor resides in the middle of the reaction medium. The beam from a helium-neon laser is used to break a chemical wave into a pair of spiral rotors. One of the rotors is then driven to the edge of the disk reactor. At high malonic acid concentrations $[(0.4\text{--}0.6)M]$, we observe a periodic (simple) rotating spiral, as shown in Fig. 1(d). The tip of the spiral follows a small circle, as indicated in Fig. 1(a).

When the malonic acid concentration is decreased across a critical value ($0.33M$) to $0.30M$, the system undergoes a transition from simple rotating spirals to meandering spirals [15–18], and the time dependence of the concentrations at any point in the reaction-diffusion medium changes from periodic to quasiperiodic. Two types of meandering motion have been observed in previous work: hypocycloid (outward flower petals) and epicycloid (inward flower petals) [15–17,19]. Under our experimental conditions, the tip follows a hypocycloid trace, as shown in Fig. 1(b). The orbit is similar to an earth-moon pattern where the primary cycle (moon) orbits the secondary cycle (earth) in one direction and rotates about its center in the opposite direction [17]. As we decrease the malonic acid concentration in the meandering regime, the diameter of the secondary circle increases and the petals of the spiral tip orbit grow. This large meandering motion is shown in Fig. 1(c). As a consequence of the Doppler effect, spiral waves in front of the spiral tip are compressed and spiral waves behind the spiral tip are dilated, as shown Fig. 1(f). The local oscillation period of the meandering spirals is

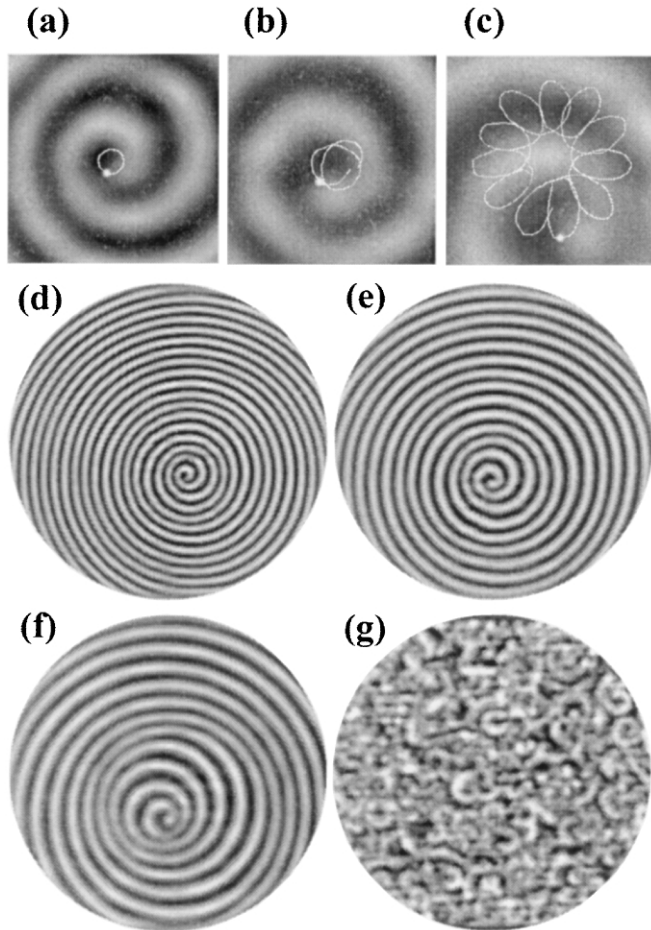


FIG. 1. Images illustrating the transition from a regular spiral to meandering spirals and to spiral turbulence as the malonic acid concentration is decreased. (a)–(c) Enlargements of the central part of (d)–(f). The white lines in (a)–(c) show the orbit of the spiral tip, and the white dots mark the location of the spiral tips in the background. Malonic acid concentrations: (a), (d) $0.40M$, simple spiral; (b), (e) $0.30M$, onset of meandering spiral; (c), (f) $0.13M$, large meandering spiral; (d) $0.10M$, spiral turbulence. Other control parameters were kept fixed: $[\text{NaBrO}_3]_0 = 0.4M$; $[\text{NaBr}]_0 = 30 \text{ mM}$; $[\text{H}_2\text{SO}_4]_0 = 0.4M$; $[\text{Ferroun}]_0 = 0.5 \text{ mM}$; residence time in each reservoir, 11 min; temperature $25 \pm 0.5 \text{ }^\circ\text{C}$. The region shown in (a)–(c) is $7.5 \times 7.5 \text{ mm}^2$; (d)–(g) 19.5 mm in diameter.

found to vary regularly in a range between a minimum and a maximum value.

The size of the petals of the spiral tip orbit increases continuously as the malonic acid concentration is decreased, so that the Doppler effect on the spiral waves becomes more and more pronounced. When the control parameter passes a second critical value ($0.12M$), the system undergoes a transition characterized by a spiral instability: spiral waves near the spiral center break and the system spontaneously generates new spiral tips (defects). This process continues until the whole system is filled with defects. Thus the asymptotic state of the system is a state of spatiotemporal turbulence, as shown in Fig. 1(g).

Figure 2 illustrates the spiral-breaking process. As the spiral tip moves toward its adjacent wave, it breaks the wave and generates a pair of defects, as shown in Figs. 2(a) and 2(b). The newly generated defects drift apart and self-organize into new spiral rotors. The daughter spirals meander in the same way as the mother; hence the daughters similarly break and generate their own daughters, as shown in Fig. 2(c). The number of spiral tips continuously increases [Fig. 2(d)] until the system is saturated with spiral defects [Fig. 1(g)].

The growth of the number of defects N as a function of time during the transition is shown in Fig. 3. The initial growth rate is almost constant. Assuming that the rate of expansion of the turbulent region into the region of spiral waves is diffusion controlled, and letting l and A , respectively, be the length and the area of the turbulent region, we have $l \propto \sqrt{t}$, so that $\frac{dA}{dt} \propto l \frac{dl}{dt} = \text{const}$. Thus Fig. 3 suggests that the average density of defects does not change when the turbulent regime invades the ordered regime, $\frac{dN}{dt} \propto \frac{dA}{dt}$. When the turbulent regime occupies the whole system, the density of defects increases [compare Fig. 2(c) with Fig. 2(d)] and the growth is no longer linear; at long times the growth in defect density stops.

The observed phenomena can be well explained by an instability mechanism that was proposed by Bär *et al.* [10]; we call it the Doppler instability. The behavior of spiral waves in an excitable medium is governed by a dispersion

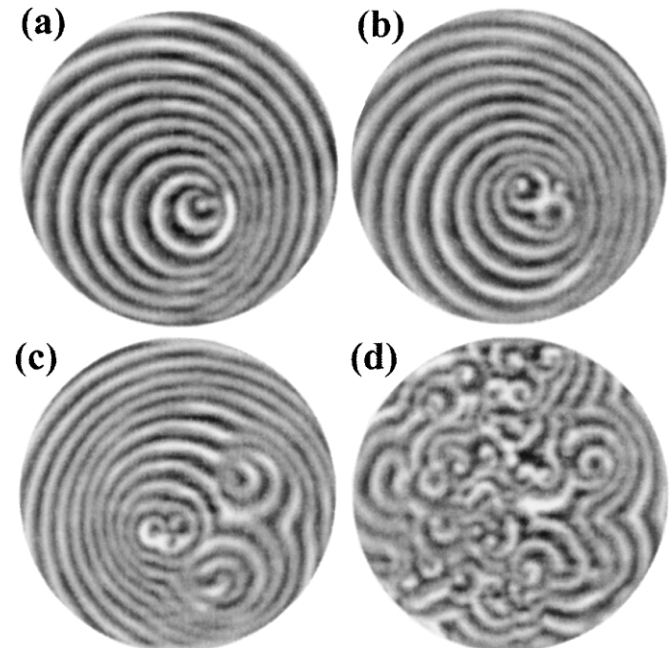


FIG. 2. The development of spiral turbulence as a single spiral undergoes a Doppler instability: (a) $t = 0$, a pair of defects was just generated; (b) $t = 100 \text{ s}$, new defects self-organize into spirals; (c) $t = 400 \text{ s}$, daughter spirals give birth to grand-daughter spirals; (d) $t = 2000 \text{ s}$, spiral turbulence. The control parameters are the same as in Fig. 1 (with $0.10M$ malonic acid concentration). The region shown is 19.5 mm in diameter.

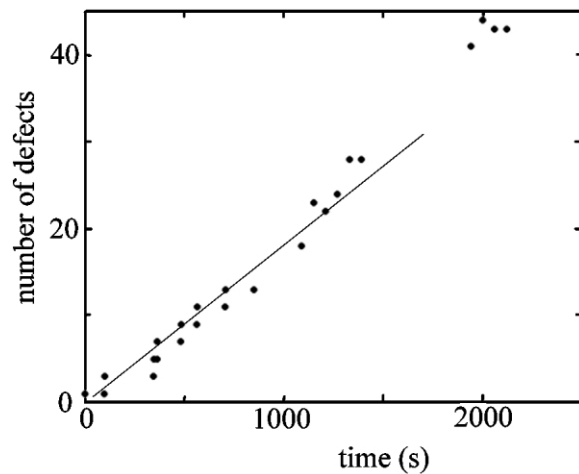


FIG. 3. The number of defects measured as a function of time during the growth of the turbulent region. The line shows the initial linear growth rate. The number of defects saturates at around 60 in about two hours.

relation that relates the speed to the period of the traveling waves. In general, the speed of the waves depends on how rapidly the local system recovers its quiescent state after being excited; hence, it is an increasing function of the period of waves [20]. There exists a minimum period p_{\min} below which the system cannot recover to its excitable state, and traveling waves cease to exist [20,21]. Generally, the period of regular spiral waves is larger than the minimum period; thus spiral waves are stable. However, when a spiral tip meanders, the local period of its waves varies because of the Doppler effect. For sufficiently large meandering, the local period of spiral waves (p_0) becomes less than p_{\min} , rendering the local chemical waves unstable, and defects are spontaneously created. Figures 2(a) and 2(b) demonstrate this process.

Figure 4 compares our experimental results with the results of a numerical simulation of Jahnke and Winfree for the Oregonator model [16], which can qualitatively describe the excitable BZ reaction [20,21]. The nondimensional two-variable Oregonator model is

$$\partial u / \partial t = (1/\varepsilon)[u - u^2 - fv(u - q)/(u + q)] + D_u \nabla^2 u$$

$$\partial v / \partial t = u - v + D_v \nabla^2 v,$$

where u , v are the two variables, f and q are constants ($0 \leq f \leq 4$, $q = 2 \times 10^{-3}$), and ε is a control parameter depending on the chemical concentrations:

$$\varepsilon = 10^{-2} \frac{[\text{BrCH}(\text{COOH})_2] + [\text{CH}_2(\text{COOH})_2]}{[\text{BrO}_3^-][\text{H}^+]}$$

If we take $f = 1.4$ as in [16] and assume that the patterned layer is located about $2/3$ of porous glass thickness from reservoir A [22], then the spiral period p_0 and the minimum period p_{\min} in Jahnke and Winfree's calculation [16] are translated into the two thin lines presented in Fig. 4. The thick line in Fig. 4 fits our experimental data for the spiral period p_0 . In the meandering spiral region

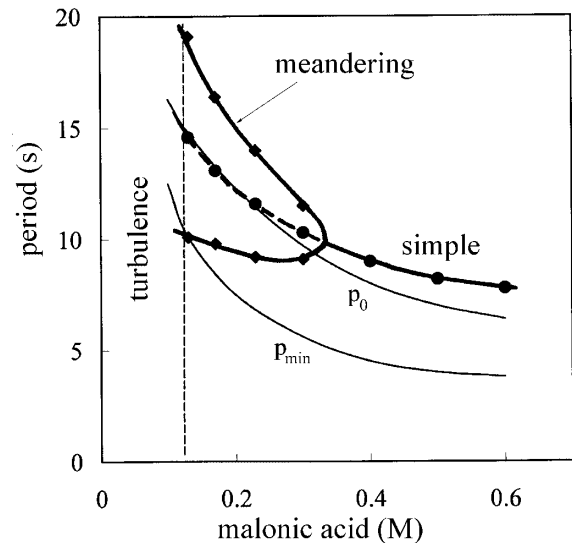


FIG. 4. Bifurcation diagram of the spiral period as a function of malonic acid concentration. The thick lines represent experimental data and the thin lines are deduced from the simulation of Jahnke and Winfree (see text). The three regimes are periodic simple rotating spirals (malonic acid $> 0.33M$), meandering spirals ($0.12M < \text{malonic acid} < 0.33M$), and defect-mediated turbulence (malonic acid $< 0.12M$).

the average values of the measured maximum and minimum period also agree with the simulations. The onset of spiral meandering occurs at a malonic acid concentration of $0.33M$. As the concentration is decreased to the second critical value ($0.12M$), the lower branch of spiral period crosses the p_{\min} line obtained in the simulation, and at the same time the system undergoes the transition from spirals to defect-mediated turbulence. Thus the observed Doppler instability is in good accord with the numerical simulation of Bär *et al.* (see Fig. 13 of Ref. [10]).

Another possible cause of the turbulence could be three-dimensional effects. Winfree [23] discusses the effect of a non-negligible thickness of a reaction medium. He observed that, if the thickness of the medium was larger than the diameter of the spiral rotor, the rotor became three-dimensional (3D). Such a rotor may spontaneously generate defects unless confined to a layer thinner than about a rotor diameter. In our experiment, as the system approaches the onset of turbulence, we indeed observe an apparent 3D effect, the bright waves visible in Fig. 2; these are caused by wave fronts curved in the z direction. However, these fronts did not break; rather, these segments are always observed to entrain, as found by Winston *et al.* [24]. Moreover, the transition to spiral turbulence occurs when the spiral wavelength becomes larger, where the spiral rotor is more confined in the z direction. At the onset of turbulence the rotor diameter is about 1 mm while the thickness of the patterned layer in the reaction medium is a fraction of 0.4 mm, much less than the rotor size.

Gray *et al.* studied the development of fibrillation in animal hearts and found that a rapid motion of spirals gives

rise to fibrillatory activity [5]. They observed a wave breaking process when the excitation wave could not proceed into the recovery region, and they estimated that there could be 15 rotors during the full development of fibrillation in a human heart [8]. These observations are consistent with the Doppler instability mechanism that we have observed in the BZ reaction. Hence, we conclude that the Doppler instability provides a plausible explanation for the onset of cardiac fibrillation.

We thank M. Bär for helpful discussions and Y. Li for assistance in data analysis. Q.O. acknowledges support from the Chinese prominent youth program. H. L. S. and G. L. acknowledge support from the Engineering Research Program of the U.S. Department of Energy Office of Basic Energy Sciences and the Robert A. Welch Foundation.

*Electronic address: qi@mail.phy.pku.edu.cn

†Electronic address: swinney@chaos.ph.utexas.edu

- [1] K. J. Lee, E. C. Cox, and R. E. Goldstein, *Phys. Rev. Lett.* **76**, 1174 (1996).
- [2] J. M. Davidenko, A. V. Pertsov, R. Salomonsz, W. Baxter, and J. Jalife, *Nature (London)* **355**, 349 (1992).
- [3] *Chemical Waves and Patterns*, edited by R. Kapral and K. Showalter (Kluwer Academic Publisher, Dordrecht, 1995), Pt. 1.
- [4] A. T. Winfree, *Science* **266**, 1003 (1994).
- [5] R. A. Gray, J. Jalife, A. V. Panfilov, W. T. Baxter, C. Cabo, J. M. Davidenko, and A. M. Pertsov, *Science* **270**, 1222 (1995).
- [6] L. Glass, *Phys. Today* **49**, No. 8, 40 (1996).
- [7] A. V. Holden, *Nature (London)* **392**, 20 (1998).
- [8] R. A. Gray, A. M. Pertsov, and J. Jalife, *Nature (London)* **392**, 75 (1998).
- [9] F. X. Witkowski, L. J. Leon, P. A. Penkoske, W. R. Giles, M. L. Spano, W. L. Ditto, and A. T. Winfree, *Nature (London)* **392**, 78 (1998).
- [10] M. Bär, M. Hildebrand, M. Eiswirth, M. Falcke, H. Engel, and M. Neufeld, *Chaos* **4**, 499 (1994).
- [11] Q. Ouyang and J.-M. Flesselles, *Nature (London)* **379**, 143 (1996).
- [12] A. Belmonte, J.-M. Flesselles, and Q. Ouyang, *Europhys. Lett.* **35**, 665 (1996).
- [13] A. Karma, *Nature (London)* **379**, 118 (1996).
- [14] Q. Ouyang and H. L. Swinney, *Chaos* **1**, 411 (1991).
- [15] D. Barkley, M. Kness, and L. S. Tuckerman, *Phys. Rev. A* **42**, 2489 (1990).
- [16] W. Jahnke and A. T. Winfree, *Int. J. Bifurcation Chaos Appl. Sci. Eng.* **1**, 445 (1991).
- [17] G. Li, Q. Ouyang, V. Petrov, and H. L. Swinney, *Phys. Rev. Lett.* **77**, 2105 (1996).
- [18] V. Hakim and A. Karma, *Phys. Rev. Lett.* **79**, 665 (1997).
- [19] V. S. Zykov, *Biophysics* **31**, 940 (1986).
- [20] J. P. Keener and J. J. Tyson, *Physica (Amsterdam)* **21D**, 307 (1986).
- [21] J. D. Dockery, J. P. Keener, and J. J. Tyson, *Physica (Amsterdam)* **30D**, 177 (1988).
- [22] Since there are multiple concentration gradients normal to the plane of the reaction medium, the value of $\frac{[\text{BrCH}(\text{COOH})_2] + [\text{CH}_2(\text{COOH})_2]}{[\text{BrO}_3^-][\text{H}^+]}$ varies in that direction. The assumption made provides the best fit to the simulation. If the patterned layer were in the middle of the reaction medium, ε would increase a factor of 2, and the calculated lines would move down about 20%.
- [23] A. T. Winfree, *Nature (London)* **371**, 233 (1994).
- [24] D. Winston, M. Arora, J. Maselko, V. Cáspar, and K. Showalter, *Nature (London)* **351**, 132 (1991).